

# The Ginsparg-Wilson relation and overlap fermions

Thomas DeGrand

*Department of Physics, University of Colorado, Boulder, CO 80309, USA\**

(Dated: March 6, 2026)

arXiv:2512.07743v2 [hep-lat] 5 Mar 2026

## Abstract

I review the physics of lattice fermions obeying the Ginsparg-Wilson relation. I describe their relation to domain wall fermions. I give a description of methodology for performing numerical simulations with overlap fermions. This is a chapter contributed to the on-line book “Lattice QCD at 50 years,” (LQCD@50), edited by Tanmoy Bhattacharya, Maarten Golterman, Rajan Gupta, Laurent Lellouch, and Steve Sharpe.

## I. INTRODUCTION AND MOTIVATION

The simplest lattice fermions have issues with chiral symmetry. The situation is encoded in a famous “no-go” theorem due to Nielsen and Ninomiya [1, 2], see also Karsten and Smit [3]. The theorem makes two assumptions:

1. There is a quadratic fermion action  $\bar{\psi}(x)iH(x-y)\psi(y)$ , where  $H(p)$  is continuous and well behaved. It should reduce to  $\gamma_\mu p_\mu$  for small  $p_\mu$ .
2. There is a local conserved charge  $Q$  defined as  $Q = \sum_x j_0(x)$ , which is quantized (i. e.  $Q$  doesn't change across the Brillouin zone)

The theorem is that, once these conditions hold,  $H(p)$  has an equal number of left handed and right handed fermions for each eigenvalue of  $Q$ : this is called “doubling.” The choices we seem to have are to work with fermion actions which are chiral but doubled (naive or staggered fermions) or undoubled but with explicit order  $a$  or  $a^2$  violations of chiral symmetry (Wilson or clover fermions).

However there is a third way to evade the theorem, which basically amounts to making a redefinition of what is called “chiral symmetry” on the lattice. Fermion actions which do this are called “Ginsparg-Wilson” actions (after their discoverers [4]) or “overlap” actions (for their particular implementation choice). They are related to “domain wall fermions,” which live in five dimensions. Domain wall fermions are described by Blum and Shamir in a separate review. The connection is also described in Sec. III of this chapter. Oddly enough, though, nearly all the technical developments of Ginsparg-Wilson fermions and domain wall fermions proceeded in an essentially decoupled way. This chapter attempts to give a stand-alone survey of lattice implementations of overlap fermions, from a description of their formal background to a discussion of issues associated with their practical implementation in simulations.

## II. FORMAL PROPERTIES OF GINSPARG-WILSON FERMIONS

Overlap (or, more generally, Ginsparg-Wilson) fermions replace [5] the usual definition of a chiral rotation  $\delta\psi = i\epsilon\gamma_5\psi$ ,  $\delta\bar{\psi} = i\epsilon\bar{\psi}\gamma_5$  by either

$$\delta\psi = i\epsilon\gamma_5 \left(1 - \frac{a}{2r_0}D\right) \psi; \quad \delta\bar{\psi} = i\epsilon\bar{\psi} \left(1 - \frac{a}{2r_0}D\right) \gamma_5 \quad (2.1)$$

---

\* thomas.degrand@colorado.edu

or

$$\delta\psi = i\epsilon\gamma_5 \left(1 - \frac{a}{r_0}D\right)\psi; \quad \delta\bar{\psi} = i\epsilon\bar{\psi}\gamma_5. \quad (2.2)$$

The operator  $D$  should be local. The lattice spacing is  $a$  and  $r_0$  is a free parameter. The naive  $a \rightarrow 0$  limit of the new chiral rotation is just the usual one, so this is just the ordinary chiral rotation modified by the addition of an irrelevant operator. In all situations I have seen,  $D$  in the rotation is taken to be the (massless) Dirac operator used in the action, so that the Lagrange density is  $\mathcal{L} = \bar{\psi}D\psi$ . Requiring  $\delta\mathcal{L} = 0$  under either of the altered chiral rotations replaces the usual anti-commutation relation of the Dirac operator and  $\gamma_5$  by the new constraint

$$0 = \gamma_5 D + D\gamma_5 - \frac{a}{r_0}D\gamma_5 D. \quad (2.3)$$

This expression is called the ‘‘Ginsparg-Wilson relation,’’ named after its discoverers [4].

Ginsparg and Wilson discovered it as a natural consequence of performing a real-space renormalization group transformation on a fermion action. Their Ginsparg-Wilson relation was  $\{\gamma_5, D\} = aD\gamma_5 R D$  where  $R$  is a local operator. This amounts to writing the chiral rotation as  $\delta\psi = i\epsilon\gamma_5(1 - aRD)\psi$ . This extension did not receive widespread use in practice.

The Ginsparg-Wilson relation can be rewritten as

$$\{\gamma_5, D^{-1}\} = \frac{a}{r_0}\gamma_5 \quad (2.4)$$

and, using  $D^\dagger = \gamma_5 D \gamma_5$ , a third version of the relation is

$$D + D^\dagger = \frac{a}{r_0}D^\dagger D. \quad (2.5)$$

Fermions obeying the Ginsparg-Wilson relation have a number of remarkable properties. First, their eigenvalues are confined to a circle of radius  $r_0/a$  in the complex plane, centered at the point  $(r_0/a, 0)$ . To see this, write the eigenvalue equation as  $D\phi = \lambda\phi$  with  $\lambda = x + iy$ . Eq. 2.5 says that  $2x = (a/r_0)(x^2 + y^2)$  or  $(x - r_0/a)^2 + y^2 = (r_0/a)^2$ . Second, if an eigenmode of  $D$  is chiral,  $\gamma_5\phi = \pm\phi$ , then  $\lambda$  is real and equal to either 0 or  $2r_0/a$ ,

$$(\gamma_5 D + D\gamma_5 - \frac{a}{r_0}D\gamma_5 D)\phi = (\pm 2\lambda \mp \frac{a}{r_0}\lambda^2)\phi, \quad (2.6)$$

so  $\lambda[2 - (a/r_0)\lambda] = 0$ .

The Hermitian Dirac operator  $H = \gamma_5 D$  is another useful object. In terms of  $H$ , Eq. (2.5) becomes

$$\gamma_5 H + H\gamma_5 = \frac{a}{r_0}H^2. \quad (2.7)$$

If an eigenstate  $|\psi\rangle$  of  $H$  is also an eigenstate of  $\gamma_5$ , then from Eqn. 2.7, its  $H$  eigenvalue must be one of the possibilities  $(0, \pm 2r_0/a)$ . Then it is an eigenstate of all four operators  $H$ ,  $H^2$ ,  $D$ , and  $\gamma_5$ . Otherwise,  $|\psi\rangle$  and  $\gamma_5|\psi\rangle$  form a two-dimensional subspace that is invariant under the action of  $H$  and  $\gamma_5$  (and consequently  $D$ ), and on which  $H$  has eigenvalues  $\pm\epsilon$ .

This is easiest to see by beginning with an eigenvector of  $H$ , which obeys  $H|\psi\rangle = \epsilon|\psi\rangle$  for  $\epsilon \neq 0$  or  $\pm 2r_0/a$ , and constructing the orthogonal state

$$|\phi\rangle = N[\gamma_5|\psi\rangle - |\psi\rangle\langle\psi|\gamma_5|\psi\rangle], \quad (2.8)$$

where  $N$  is a normalization factor,  $1/N^2 = 1 - |\langle \psi | \gamma_5 | \psi \rangle|^2$ . (The construction assumes that  $|\psi\rangle$  is not an eigenstate of  $\gamma_5$ .) Computing  $H|\phi\rangle$  and using the Ginsparg-Wilson relation, Eq. (2.7), we get

$$H|\phi\rangle = -\epsilon|\phi\rangle + |\psi\rangle N\epsilon \left( \epsilon \frac{a}{r_0} - 2\langle \psi | \gamma_5 | \psi \rangle \right). \quad (2.9)$$

So we see that the subspace is invariant under  $H$ . From this we learn that  $|\phi\rangle$  is an eigenstate of  $H$  with eigenvalue  $-\epsilon$  and (because  $H$  is Hermitian)  $\langle \psi | \gamma_5 | \psi \rangle = \epsilon/(2r_0/a)$ . Finally, we see that  $H^2$  is just  $\epsilon^2$  on this subspace and it commutes with  $\gamma_5$ , so we can diagonalize  $H^2$  and  $\gamma_5$  simultaneously.

In a basis where  $\gamma_5 = \text{diag}(+1, -1)$ , we can write

$$\psi = \begin{pmatrix} \alpha \\ \beta \end{pmatrix} = \frac{1}{\sqrt{2}} \begin{pmatrix} \sqrt{1 + \frac{\epsilon a}{2r_0}} \\ \sqrt{1 - \frac{\epsilon a}{2r_0}} \end{pmatrix}. \quad (2.10)$$

This allow us to write down  $H$  in the simultaneous eigenbasis of  $H^2$  and  $\gamma_5$ . It is a direct sum of two by two blocks, each of which is

$$H = \frac{1}{2r_0/a} \begin{pmatrix} \epsilon^2 & \epsilon\sqrt{(2r_0/a)^2 - \epsilon^2} \\ \epsilon\sqrt{(2r_0/a)^2 - \epsilon^2} & -\epsilon^2 \end{pmatrix}. \quad (2.11)$$

In addition  $H$  may have simple diagonal terms for  $\epsilon = 0$  or  $2r_0/a$ .

This seems formal but it is quite useful when one wants to find eigenfunctions of  $D$  or  $H$ : the spectrum of  $H^2$  is bounded from below, so numerical methods which find the lowest eigenvalue eigenmodes of a matrix can be used, and one can construct as much of the spectrum as one wants working in a single chirality basis. Typically, this is the sector which contains all the zero modes.

The operator  $D = \gamma_5 H$  reduces, of course, to block-diagonal form on the same two- or one-dimensional eigenspaces of  $H^2$ . Where the eigenvalues of  $H$  are  $\pm\epsilon$ , the eigenvalues of  $D$  come in complex conjugate pairs,

$$\lambda = \frac{\epsilon^2 \pm i\epsilon\sqrt{(2r_0/a)^2 - \epsilon^2}}{2r_0/a}, \quad (2.12)$$

or they are real:  $\epsilon = 0$  corresponds to  $\lambda = 0$  and  $\epsilon = \pm 2r_0/a$  corresponds to  $\lambda = 2r_0/a$ . Where eigenmodes of  $H$  with nonzero eigenvalue  $\pm\epsilon$  have matrix elements  $\langle \phi | \gamma_5 | \phi \rangle = \pm\epsilon/(2r_0/a)$ , from Eq. 2.3 it is easy to show that nonzero eigenvalue eigenmodes of  $D$  have  $\langle \psi | \gamma_5 | \psi \rangle = 0$ .

Since the Hilbert space of Dirac fields is complete and finite dimensional it must be that  $\text{Tr } \gamma_5 = 0$ . Taking the trace on the eigenbasis of  $D$ , we find that the only nonzero contributions come from the eigenspaces 0 and  $2r_0/a$ . In the eigenspace 0,  $\text{Tr } \gamma_5$  counts the difference  $n_+ - n_-$  between zero eigenmodes of positive and negative chirality. In the eigenspace  $2r_0/a$  it counts the corresponding difference  $n'_+ - n'_-$ . For the net trace to vanish, we must have  $(n_+ - n_-) + (n'_+ - n'_-) = 0$ . Similar reasoning shows that  $\text{Tr } \gamma_5 D = (2r_0/a)(n'_+ - n'_-)$ . This leads us to the identity

$$Q = \frac{a}{2r_0} \text{Tr } \gamma_5 D = -\text{Tr } \gamma_5 \left( 1 - \frac{a}{2r_0} D \right) = n_- - n_+. \quad (2.13)$$

This is the first part of the index theorem, which equates the topological charge (winding number) to  $Q$ , the difference between the numbers of zero eigenmodes of positive and negative chirality, gauge configuration by configuration. To complete the theorem it is necessary to relate  $Q$  to the topological charge. For a smooth background gauge configuration, showing that  $\text{Tr } \gamma_5 D$  is proportional to the integral over  $\epsilon^{\alpha\beta\mu\nu} F_{\alpha\beta}^a F_{\mu\nu}^a$  involves manipulations similar to what is done in the continuum calculation (and for that, see the text [6]).

It is convenient to define the massive overlap operator for fermion mass  $m$  as

$$D(m) = \left(1 - \frac{m}{2r_0/a}\right) D + m. \quad (2.14)$$

With this definition, (naturally  $H(m) = \gamma_5 D(m)$ ),

$$D(m)^\dagger D(m) = H(m)^2 = \left[1 - \frac{m^2}{4(r_0/a)^2}\right] H^2 + m^2. \quad (2.15)$$

The ‘‘shifted propagator’’  $\hat{D}(m)^{-1}$  is often used in calculations:

$$\left(1 - \frac{m}{2r_0/a}\right) \hat{D}(m)^{-1} = D(m)^{-1} - \frac{1}{2(r_0/a)}. \quad (2.16)$$

It obeys

$$\{\gamma_5, \hat{D}(m)^{-1}\} = 2m\hat{D}(m)^{-1}\gamma_5\hat{D}(m)^{-1}. \quad (2.17)$$

$\hat{D}$ , the inverse shifted propagator, is generally not local, but its anti-commutator is quite familiar:  $\{\gamma_5, \hat{D}\} = 2m\gamma_5$ . One could not ask for anything more chiral than this.

For the domain wall story about  $\hat{D}(m)^{-1}$ , see the chapter by Blum and Shamir, Sec. 4.5.

Eq. 2.17 immediately gives us  $m_{PS}^2 \propto m_q$ : multiply both sides on the left by  $\gamma_5$ , trace and sum over sites,

$$2\text{Tr}\hat{D}^{-1} = 2m\text{Tr}\gamma_5\hat{D}(m)^{-1}\gamma_5\hat{D}(m)^{-1}. \quad (2.18)$$

The right hand side has the topology of a flavor nonsinglet pseudoscalar correlator. Eq. 2.18 can be written as

$$\frac{1}{V} \sum_x \langle S(x) \rangle = \frac{m_q}{V} \sum_{x,y} \langle P(x)P(y) \rangle \quad (2.19)$$

with the scalar and pseudoscalar currents defined (to leading order in  $m$ ) as

$$S = \bar{q}(x,t)\left(1 - \frac{a}{2r_0}D\right)q(x,t); \quad P = \bar{q}(x,t)\left(1 - \frac{a}{2r_0}D\right)\gamma_5 q(x,t). \quad (2.20)$$

When chiral symmetry is broken, the left hand side of Eq. 2.19 is the chiral condensate  $\Sigma$ . Saturating the correlator on the right hand side of Eq. 2.19 with the pseudoscalar state gives us

$$C(t) = \sum_{\vec{x}} \langle P(\vec{x},t)P(0,0) \rangle = |\langle 0|P|PS \rangle|^2 \frac{\cosh(m_{PS}(N_t/2 - t))}{2m_{PS} \sinh(m_{PS}N_t/2)}. \quad (2.21)$$

and its integral over the simulation volume is

$$\int_0^{N_t} dt C(t) = \frac{|\langle 0|P|PS \rangle|^2}{m_{PS}^2}. \quad (2.22)$$

When  $\Sigma$  is nonzero this gives us

$$\frac{|\langle 0|P|PS\rangle|^2}{m_{PS}^2} = \frac{\Sigma}{m_q}. \quad (2.23)$$

which is  $m_{PS}^2 \propto m_q$ .

Chiral Ward identities come from writing Eq. 2.17 as

$$\hat{D}(m)^{-1} + \gamma_5 \hat{D}(m)^{-1} \gamma_5 = 2m \gamma_5 \hat{D}(m)^{-1} \gamma_5 \hat{D}(m)^{-1} \quad (2.24)$$

so

$$\begin{aligned} \text{Tr} \hat{D}(m)^{-1} \Gamma \hat{D}(m)^{-1} \Gamma + \text{Tr} \hat{D}(m)^{-1} \Gamma (\gamma_5 \hat{D}(m)^{-1} \gamma_5) \Gamma \\ = 2m \text{Tr} \hat{D}(m)^{-1} \Gamma (\gamma_5 \hat{D}(m)^{-1} \gamma_5 \hat{D}(m)^{-1} \gamma_5) \Gamma \end{aligned} \quad (2.25)$$

for any gamma matrix  $\Gamma$ . For  $\Gamma = \gamma_\mu$  this is the vector - axial vector - pseudoscalar Ward identity

$$\langle V_\mu V_\mu \rangle - \langle A_\mu A_\mu \rangle = 2m \langle A_\mu P V_\mu \rangle. \quad (2.26)$$

for

$$V_\mu = \bar{q}(x, t) \left(1 - \frac{a}{2r_0} D\right) \gamma_\mu q(x, t); \quad A_\mu = \bar{q}(x, t) \left(1 - \frac{a}{2r_0} D\right) \gamma_\mu \gamma_5 q(x, t). \quad (2.27)$$

None of the currents we have defined are Noether currents, so there will be matching factors connecting them to their continuum analogs. The continuum Ward identities are identical to the ones we have written. Eq. 2.26, plus the corresponding one with  $\Gamma = 1$ , tell us that lattice to continuum matching factors for the vector and axial currents are equal, as are those for the scalar and pseudoscalar currents,  $Z_V = Z_A$ ,  $Z_P = Z_S$ .

Notice that the extra terms in the currents and identities compared to the continuum relations involve the product  $D^{-1}D$ , which is a contact term in the correlation functions.

The singlet analog of Eq. 2.18 includes the topological charge and gives the Di Vecchia and Veneziano [7], Leutwyler and Smilga [8], and Crewther [9] relation, that the topological susceptibility vanishes linearly with the fermion mass. For details, see (for example) the early review by Niedermeyer [10].

This is all very magical: we have a lattice fermion whose chiral properties are equal (up to contact terms) to those of continuum fermions, without doubling. To quote from a letter to the author from Peter Hasenfratz: “It is like opening Pandora’s box.”

The final issue is, what is an explicit formula for a Dirac operator which obeys the Ginsparg-Wilson relation? One last definition gives a clue: Because the eigenvalues of  $D$  lie on a shifted circle, one can write  $D$  as

$$D = \frac{r_0}{a} [1 + V] \quad (2.28)$$

where  $V$  is a unitary operator. We can choose  $V$  to be a function of some ordinary, nonchiral, undoubled massless lattice Dirac operator  $d$  (referred to hereafter as the “kernel” Dirac operator) and a mass term equal to  $-r_0/a$ . The universally-used choice of function is the overlap action of Refs. [11, 12]

$$D = \frac{r_0}{a} \left[ 1 + \frac{d - r_0/a}{\sqrt{(d - r_0/a)^\dagger (d - r_0/a)}} \right] \quad (2.29)$$

or, introducing the Hermitian operator  $h(m) = \gamma_5(d + m)$ ,

$$D = \frac{r_0}{a}[1 + \gamma_5\epsilon[h(-r_0/a)]] \quad (2.30)$$

where  $\epsilon(h)$  is the matrix step function,  $\epsilon(h) = h/\sqrt{h^2}$ . The choice of coefficients is made for convenience so that the small eigenvalue limit the overlap operator has the same normalization as the kernel operator  $D \simeq d \simeq i\cancel{D}$ .

All magical things have a high price. Here, the problem is that  $V$  is not restricted to extend over a finite number of lattice sites. Said another way, it is not ultralocal. This means that the matrix representation of  $D$  is not sparse.

There was a theoretical issue in the literature: was  $D$  local? ‘‘Locality’’ means that the size of  $D(|x - y|)$  dies exponentially with the separation  $|x - y|$ ,  $D \propto \exp(-C|x - y|)$ . Here  $|x - y|$  is a distance measured in lattice units; the physical distance is  $r = a|x - y|$  and  $D \propto \exp(-Cr/a)$  vanishes when  $r \gg a$ . The answer to this question depended on the choice of the kernel. A proof of locality when the kernel  $d$  was the Wilson action with thin links, but in the limit of very smooth gauge fields, was presented in Ref. [13]. Most of the literature involved issues related to using the Wilson action as a kernel. I never did that, so for me the only issue of principle is illustrated in Fig. 1. The overlap maps  $d$  into a circle. All of the eigenmodes of  $d$  with real eigenvalues closer to the origin than the value of  $r_0/a$  will be pushed to the origin and act as separate flavors. We don’t want doubling, so there had better only be one set of these modes. In the figure, it had better be that  $r_0/a < 1$ . This was never an issue in practice to maintain. Also, in practice,  $C$  was never known from first principles, so everybody who ever simulated overlap fermions looked at a plot of something like  $D(x - y)\delta(y)$  as a function of  $|x - y|$  and tuned  $d$  and  $r_0$  to minimize the range of  $D$ .

This takes us (after a brief aside) to Sec. IV, which is a discussion of practical considerations: how to construct the overlap  $D$  (and related quantities) as efficiently as possible.

### III. THE OVERLAP ACTION BEGINNING IN FIVE DIMENSIONS

We pause to return to the discussion of chiral fermions in five dimensions. Let us re-state some conventions: the coordinate in the fifth dimension is  $s$ , and the five-dimensional Dirac operator  $D_5$  is written in terms of a four dimensional Dirac operator  $D_4$  and a mass function  $M(s)$  as

$$D_5 = D_4 + \gamma_5\partial_5 - M(s). \quad (3.1)$$

Since the situation does not depend on a particular form for  $M$ , let us replace it by a wall with Dirichlet boundary conditions at  $s = 0$ . We restrict ourselves to  $s > 0$  and take  $M(s) = M$  in that domain. For this simplified case the left-handed zero mode is pinned to the  $s = 0$  surface and its wave function falls away like  $\exp(-Ms)$ . Now let us find the four dimensional effective field theory of the massless mode. We can do this by finding the propagator  $G(x, s; y, s_0)$  between two sites in the five-dimensional manifold and restrict our attention to the case  $s = s_0 = 0$  (since that is where the massless mode is confined).

The Green’s function obeys

$$D_5G(x, s; y, s_0) = \delta^4(x - y)\delta(s - s_0) \quad (3.2)$$

with the boundary conditions that  $G(x, s; y, s_0)$  should vanish as  $|s - s_0|$  goes to infinity and

$$P_+G(x, s; y, s_0) = 0 \quad (3.3)$$

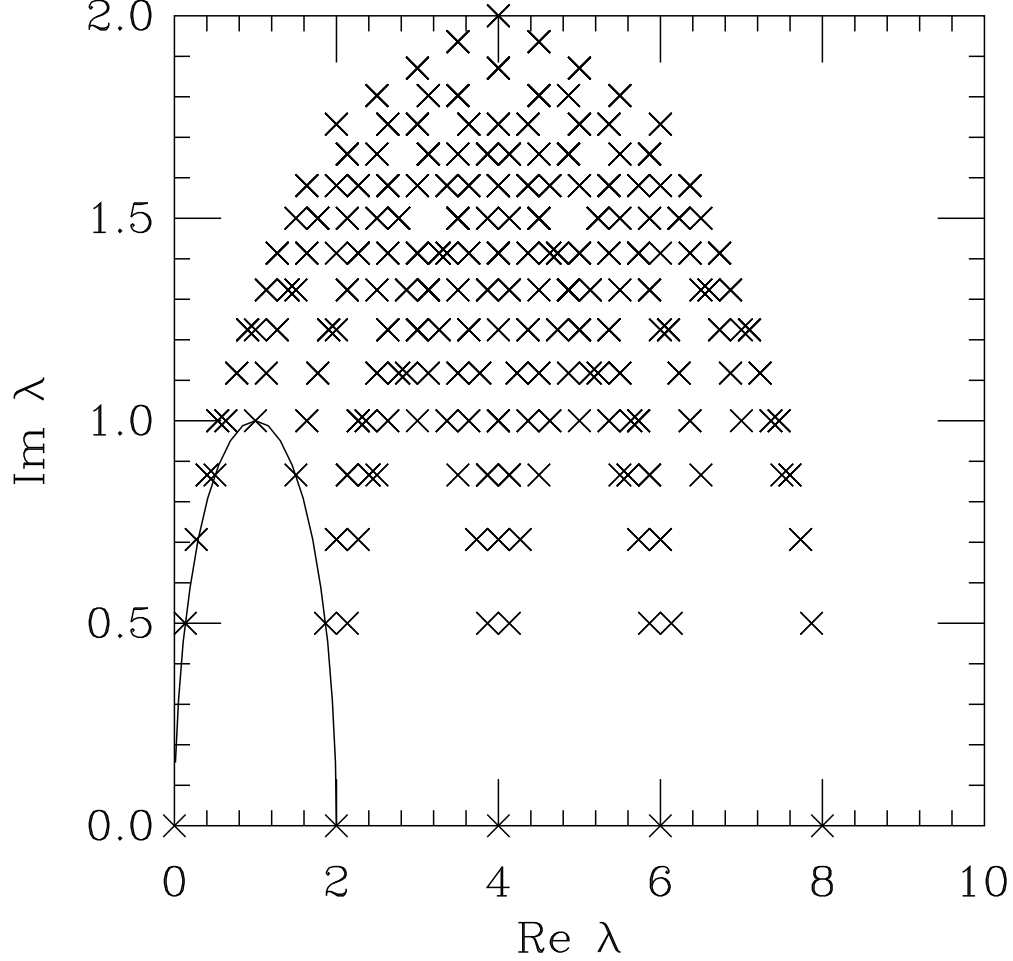


FIG. 1. A comparison of the spectrum of eigenvalues of the ordinary Wilson fermion action (crosses) on a finite lattice, with the corresponding spectrum of an  $r_0/a = 1$  overlap action (the line).

at  $s = 0$ . Here I introduce the chiral projectors

$$P_{\pm} = \frac{1}{2}(1 \pm \gamma_5). \quad (3.4)$$

A few more definitions are useful before we proceed. First, set

$$Q = \gamma_5(M - D_4) \quad (3.5)$$

so

$$D_5 = \gamma_5(\partial_5 - Q). \quad (3.6)$$

To make contact with the notation of previous sections,  $M = r_0/a$ ,  $D_4 = d$  is the kernel operator and  $Q = -h(-r_0/a)$  is the Hermitian Dirac operator. Eigenmodes of  $Q$ ,

$$Q |n\rangle = q_n |n\rangle, \quad (3.7)$$

will be used to construct the solution. Positive and negative eigenvalue projectors of  $Q$ ,

$$\begin{aligned}\hat{P}_\pm &= \frac{1}{2}\left(1 \pm \frac{Q}{\sqrt{Q^2}}\right) \\ &\equiv \frac{1}{2}(1 \pm \epsilon(Q)),\end{aligned}\tag{3.8}$$

will play a rôle in what follows.

Our goal is to show that

$$G(x, s = 0; y, s_0 = 0) = 2MP_-S(x, y)P_+, \tag{3.9}$$

where  $S(x, y) = D_{ov}(x, y)^{-1}$  if  $x \neq y$ , with

$$D_{ov} = M[1 - \gamma_5\epsilon(Q)]. \tag{3.10}$$

That is,  $D_{ov}$  is the overlap Dirac operator. The derivation of this result was first given by Lüscher [14].

To begin, write the four dimensional delta function in terms of the eigenmodes of  $Q$

$$\delta^4(x - y) = \sum_n \langle x|n\rangle \langle n|y\rangle \tag{3.11}$$

and likewise write the Green's function as

$$G(s, x; s_0, y) = \sum_n \langle x|n\rangle \mathcal{G}_n(s, s_0) \langle n|y\rangle. \tag{3.12}$$

Then  $\mathcal{G}_n(s, s_0)$  obeys the differential equation

$$\gamma_5(\partial_5 - q_n)\mathcal{G}_n(s, s_0) = \delta(s - s_0). \tag{3.13}$$

Leaving aside the boundary conditions for the moment, the solution to this simple problem is

$$\begin{aligned}\mathcal{G}_n(s, s_0) &= [Ae^{q_n(s-s_0)}]\gamma_5 && \text{if } s < s_0 \\ &= [Be^{q_n(s-s_0)}]\gamma_5 && \text{if } s > s_0\end{aligned}\tag{3.14}$$

where  $B - A = 1$  to handle the discontinuity due to the delta function. At this point we can write the Green's function as

$$G(s, x; s_0, y) = \sum_n \langle x|n\rangle e^{q_n s}[\theta(s - s_0) + C]e^{-q_n s_0}\gamma_5 \langle n|y\rangle. \tag{3.15}$$

(I have split the  $\langle x|n\rangle$  and  $\langle n|y\rangle$  apart because at the end I will want to write the answer directly in terms of operators depending on  $Q$ .)

Now for the boundary conditions. We want the solution to fall to zero as  $|s - s_0|$  goes to infinity. Make the replacement

$$\theta(s - s_0) = \theta(s - s_0)(\hat{P}_+ + \hat{P}_-) \tag{3.16}$$

in Eq. 3.15. The  $\hat{P}_-$  part of this expression gives a contribution to the Green's function which falls to zero at big  $|s - s_0|$ . To handle the positive eigenmodes, write

$$\theta(s - s_0)\hat{P}_+ = -(1 - \theta(s - s_0))\hat{P}_+ + \hat{P}_+. \quad (3.17)$$

Now we have

$$\begin{aligned} G(s, x; s_0, y) = & \sum_n \langle x|n\rangle e^{qn s} [\theta(s - s_0)\hat{P}_- \\ & - (1 - \theta(s - s_0))\hat{P}_+ + (\hat{P}_+ + C)] e^{-qn s_0} \gamma_5 \langle n|y\rangle. \end{aligned} \quad (3.18)$$

or

$$G(s, x; s_0, y) = \sum_n \langle x|n\rangle e^{qn s} [\theta(s - s_0)\hat{P}_- - \theta(s_0 - s)\hat{P}_+ + C'] e^{-qn s_0} \gamma_5 \langle n|y\rangle. \quad (3.19)$$

The first two terms satisfy the desired boundary condition at large  $|s - s_0|$ . To make sure that the  $C'$  term also obeys the boundary condition, we need  $C' = \hat{P}_- O \hat{P}_+$  for some  $O$ . We have arrived at

$$\begin{aligned} G(s, x; s_0, y) = & \sum_n \langle x|n\rangle e^{qn s} [\theta(s - s_0)\hat{P}_- \\ & - \theta(s_0 - s)\hat{P}_+ + \hat{P}_- O \hat{P}_+] e^{-qn s_0} \gamma_5 \langle n|y\rangle. \end{aligned} \quad (3.20)$$

Now we take the limit  $s \rightarrow 0$  first, then  $s_0 \rightarrow 0$ . In everything we have done so far, the  $\hat{P}_\pm$ 's were functions of the  $q_n$ 's, but we can now interpret them as functions of the  $Q$ 's (which are themselves functions of the four dimensional coordinates) and strip off the explicit dependence on the eigenmodes of  $Q$ . Suppressing the labels  $s$  and  $s_0$ , our Green's function is

$$G(x, y) = [-\hat{P}_+ + \hat{P}_- O \hat{P}_+] \gamma_5. \quad (3.21)$$

On to the last boundary condition, Eq. 3.3. This is

$$(-P_+ + P_+ \hat{P}_- O) \hat{P}_+ = 0 \quad (3.22)$$

We use

$$P_+ \hat{P}_- = \frac{1}{2}(1 + \gamma_5) \frac{1}{2}(1 - \epsilon) = \frac{1}{2}(1 + \gamma_5) \frac{1}{2}(1 - \gamma_5 \epsilon) = P_+ \frac{D_{ov}}{2M} \quad (3.23)$$

which says that

$$O = \frac{2M}{D_{ov}}. \quad (3.24)$$

The Green's function is

$$G(x, y) = [-\hat{P}_+ + \hat{P}_- \frac{2M}{D_{ov}} \hat{P}_+] \gamma_5. \quad (3.25)$$

Finally, the improbable identities (for the student to check!)  $\epsilon(Q)(M/D_{ov}) = \gamma_5(M/D_{ov} - 1)$ ,  $(M/D_{ov})\epsilon(Q)\gamma_5 = \epsilon\gamma_5 + M/D_{ov}$ , and  $\epsilon(Q)(M/D_{ov})\epsilon(Q)\gamma_5 = \gamma_5(M/D_{ov})$  give

$$G(x, y) = P_- + P_- \frac{2M}{D_{ov}} P_+. \quad (3.26)$$

which is what we wanted to show. The  $P_-$  term is a contact term, and we can neglect it.

#### IV. NUMERICAL METHODS FOR OVERLAP FERMIONS

Let's write down the overlap operator one more time and look at it from the point of view of a programmer who wants to write efficient code to evaluate its action on a trial vector:

$$D = r_0[1 + \gamma_5 \epsilon(h(-r_0))]. \quad (4.1)$$

Again,  $h(-r_0) = \gamma_5(d - r_0)$  is a kernel Hermitian Dirac operator and  $\epsilon(x) = x/\sqrt{x^2}$  is the matrix step function. Evaluating  $\epsilon(h)$  is the real bottleneck to using the overlap operator in a simulation.

One can approximate  $\epsilon(h)$  either as a polynomial or as a rational function in  $h$ . A polynomial approximation is a power series

$$\epsilon(h) = h s_N(h^2) = h \sum_{n=0}^N c_n h^{2n}, \quad (4.2)$$

where  $s_N(x)$  is an approximation to  $1/\sqrt{x}$ . This can be (and has been) implemented as a series expansion in Chebychev polynomials  $T_n(x)$ ,

$$s_N(x) = \sum_n c_n T_n(x). \quad (4.3)$$

Diagonal rational functions are more efficient. In this case we write

$$\begin{aligned} \epsilon_N(h) &= h \frac{\sum a_n h^{2n}}{\sum b_n h^{2n}} \\ &= h \left[ c_0 + \sum_{j=1}^N \frac{c_j}{h^2 + d_j} \right], \end{aligned} \quad (4.4)$$

where the  $c$ 's and  $d$ 's are related to the  $a$ 's and  $b$ 's. The second expression in Eq. 4.4 is the one which is always used, since the sum of inverses can be computed using a multishift conjugate gradient algorithm.

For real  $x$ , any approximate  $\epsilon_N(x)$  will have a range  $0 < x_{\min} < x < x_{\max}$  where it works reasonably well, but outside that range, it will fail. These end points can be adjusted by a multiplicative change of scale, but the lower end point is never zero. In order that  $\epsilon_N(x)$  is to be a good approximation to the  $\epsilon(h)$  we need for the overlap, it must be that the good interval contains all the eigenvalues of  $h$  from the smallest (absolute value)  $|\lambda_{\min}|$  to largest  $|\lambda_{\max}|$ . The largest eigenvalue is bounded by the lattice cutoff, so in typical simulations, its value is very stable. As usual, the smallest eigenvalue is the problematic one. Indeed, in a dynamical simulation,  $\lambda_{\min}$  will cross the origin when the topology of the gauge configuration changes, so one will always encounter arbitrarily small values of  $\lambda$ .

The cure to this problem is to isolate the small eigenvalue eigenmodes and include their contributions exactly. Find them and sort the eigensolutions  $h(-r_0)|j\rangle = \lambda_j|j\rangle$  in order from the smallest  $|\lambda_0|$  to largest  $|\lambda_{\max}|$ . Then apply  $\epsilon(h)$  to a vector  $|\psi\rangle$  as follows:

$$\epsilon(h)|\psi\rangle = \epsilon_N(h) \left( |\psi\rangle - \sum_{j=1}^J |j\rangle \langle j|\psi\rangle \right) + \sum_{j=1}^J |j\rangle \epsilon(\lambda_j) \langle j|\psi\rangle. \quad (4.5)$$

Now  $\epsilon_N(h)$  has to be a good approximation only for the range  $|\lambda_{J+1}|$  to  $|\lambda_{\max}|$ .

Clearly, some tuning is involved to find an optimum choice of parameters. Eigenfunctions and eigenvalues of  $h$  have to be found; this is done by finding a set of low-lying spectrum of  $h^2$  (which is bounded from below) and then diagonalizing  $h$  in the eigenbasis. This is expensive and the cost grows as more and more eigenmodes are needed. Then one must find a good combination of  $c_j$ ,  $d_j$  and  $N$  in Eq. 4.4 and  $J$  in Eq. 4.5 to insure that the step function is being evaluated to some desired accuracy and at minimum cost.

This can be tested in simulation in several ways. One can ask whether  $D$  or  $H$  have chiral zero modes (zero eigenvalue at the level of desired precision) on sample gauge configurations, such as ones with an isolated instanton. One can ask the same question, but on gauge fields in the ensemble one hopes to use for physics. Generally, this is a more stringent test, since the rougher the gauge configuration, the harder it is for an approximation to the overlap to capture its properties. Finally, one can check that one's results encode chiral symmetry, either by checking that the squared pion mass vanishes at zero bare quark mass, or by observing the absence of additive mass renormalization via a measurement of the Axial Ward Identity fermion mass involving the axial current and the pseudoscalar current,

$$\partial_t \sum_{\vec{x}} \langle A_0(\vec{x}, t) O(0, 0) \rangle = 2am_q^{AWI} \sum_{\vec{x}} \langle P^a(\vec{x}, t) O(0, 0) \rangle. \quad (4.6)$$

This choice is easier to implement and interpret.

Two examples of  $\epsilon_N$ 's are the polar expression and the Zolotarev approximation. The polar expression [referring to Eq. (4.4)] has  $c_0 = 0$  and

$$c_k = \frac{1}{N \cos^2 \left[ \pi(k - \frac{1}{2})/2N \right]}; \quad d_k = \tan^2 \left[ \pi(k - \frac{1}{2})/2N \right] \quad (4.7)$$

It is actually the power series expansion of the approximate step function used by the ordinary finite-fifth-dimension domain wall fermion. In my experience, it is not robust enough to use in most situations.

The Zolotarev formula represents the state of the art. Referring readers to the mathematical literature (see [15, 16]) for its derivation, I simply present the recipe for its implementation. The coefficients are defined in terms of the elliptic integrals  $\text{cel}$ ,  $\text{cn}$ ,  $\text{sn}$ , and  $\text{dn}$ , which I will list due to the multitude of conventions (I am following those of Ref. [17]): The approximate step function is

$$\epsilon_N(x) = x \sum_{\ell=1}^N \frac{b_\ell}{x^2 + c_{2\ell-1}}. \quad (4.8)$$

For  $x \in (x_{\min}, x_{\max})$  define  $\kappa = x_{\min}/x_{\max}$ ;  $\kappa_p = \text{cel}(\kappa, 1, 1, 1)$ ; and  $u = \ell\kappa_p/(2N)$ . Then the partial fraction coefficients are

$$c_\ell = \left[ \frac{\text{sn}(u, \kappa^2)}{\text{cn}(u, \kappa^2)} \right]^2 x_{\min}^2$$

$$b_\ell = \frac{\prod_{i=1}^{N-1} (c_{2i} - c_{2\ell-1})}{\prod_{i=1, i \neq \ell}^N (c_{2i-1} - c_{2\ell-1})}. \quad (4.9)$$

The elliptic integrals are

$$\begin{aligned}
\text{cel}(k, p, a, b) &= \int_0^\infty \frac{a + bx^2}{(1 + px^2)\sqrt{(1 + x^2)(1 + k^2x^2)}} dx \\
y &= \text{sn}(u, k) \\
u &= \int_0^{\text{sn}} \frac{dy}{\sqrt{(1 - y^2)(1 - k^2y^2)}}
\end{aligned} \tag{4.10}$$

with  $\text{sn}^2 + \text{cn}^2 = 1$ ,  $k^2\text{sn}^2 + \text{dn}^2 = 1$ .

The extrema of  $\epsilon_N$  are located at  $x_1 = x_{\min}$  and  $x_2 = x_{\min}/\text{dn}[\kappa_p/(2N)]$ . The resulting  $\epsilon_N(x)$  needs a small correction to remove an asymmetric deviation from  $\epsilon(x) = 1$ . There does not seem to be a preferred minimization criterion (absolute deviation, least squares, etc.) in the literature. Replacing  $b_\ell$  by  $2b_\ell/|\epsilon_N(x_1) + \epsilon(x_2)|$  to find the smallest absolute deviation is a good practical choice. The precision of the resulting approximation is

$$\frac{|\epsilon_N(x_1) - \epsilon(x_2)|}{|\epsilon_N(x_1) + \epsilon(x_2)|} \tag{4.11}$$

over the desired range, so it is straightforward to pick a desired accuracy for a known range simply by varying  $N$ . We illustrate an example of a Zolotarev approximation in Fig. 2.

Incidentally, the Zolotarev formula can be used to compute  $1/\sqrt{D^\dagger D}$ , needed in the RHMC algorithm for simulating a single flavor of Wilson-type fermions. The OpenQCD package does this for the strange quark in its  $2 + 1$  flavor simulations.

Evaluating the squared Hermitian overlap operator  $H^2 = (\gamma_5 D)^2 = D^\dagger D$  underpins essentially all numerical work with the overlap. Recall that  $H^2$  commutes with  $\gamma_5$  and its eigenvectors can be chosen with definite chirality. It is convenient to make use of the chiral projections ( $P_\pm = \frac{1}{2}(1 \pm \gamma_5)$ ) so that the massive squared Hermitian overlap operator, with the usual convention for the mass terms, is  $H(m)^2 = H_+(m)^2 + H_-(m)^2$  where

$$H_\pm^2(m) = P_\pm H^2(m) P_\pm = 2 \left[ \left( \frac{r_0}{a} \right)^2 - \frac{m^2}{4} \right] P_\pm (1 \pm \epsilon(h)) P_\pm + m^2 P_\pm . \tag{4.12}$$

Calculations of the eigenmodes and eigenvalues of  $H$  can be found by using the  $m = 0$  version of Eq. 4.12. The full propagator will need  $m \neq 0$ , of course. In either case the source has to have a definite chirality.

Eigenmodes and eigenvalues of  $H$  have a literature of their own. I have had good success with two methods to find eigenmodes and eigenvalues of  $H$ . One is an implementation of the Ritz variational method as described by the authors of Ref. [18] and the other is the ‘‘primme’’ package of Refs. [19, 20].

Two examples of problems addressed by eigenvalues of  $H$  are the topological susceptibility, which can be computed just by counting zero modes of  $H$ , and calculations of parameters of the chiral Lagrangian which describes the low energy limit of QCD.

Overlap fermions are particularly suited to a limit of QCD called the ‘‘epsilon regime’’ [21, 22]. This is a situation involving a finite volume  $V = L^3$  and a quark mass so light that  $m_\pi L \ll 1$  while  $ML \gg 1$  for all other hadrons. The partition function is dominated by the pions. Everything else is massive and their contribution to the partition function is exponentially suppressed. In that limit there is a connection between eigenvalues of the Dirac operator (typically in fixed sectors of topology) and random matrix theory. The first

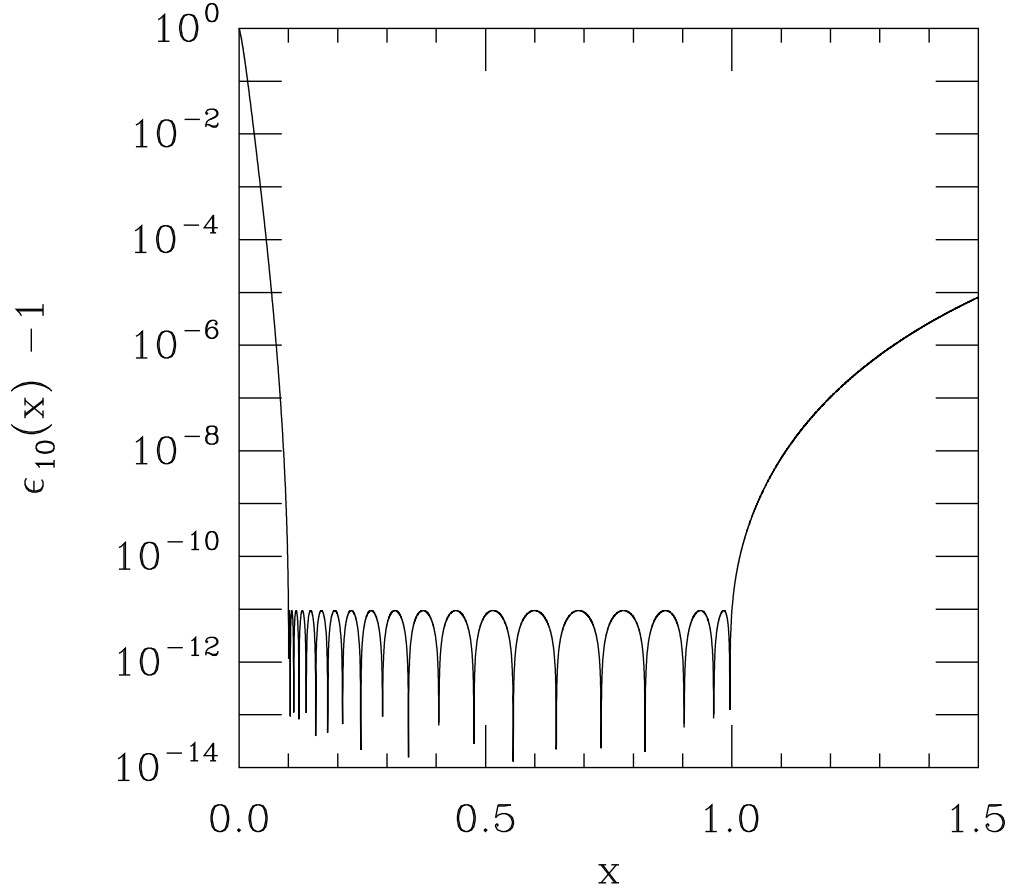


FIG. 2. An example of a tenth-order Zolotarev approximation to the step function, where the desired range is for  $0.1 < x < 1$ . We plot  $\epsilon_{10}(x) - 1$  to display the error in the approximation.

description of this connection was by Shuryak and Verbaarschot [23] and there is a large subsequent literature. An old review by Damgaard [24] is still a good introduction to the subject. The most recent discussion of this topic is probably the 2019 FLAG review [25]. In a sentence, the probability distribution of Dirac eigenvalues can be used to determine the condensate and other low energy constants of the chiral Lagrangian.

The advantage of using the overlap as opposed to other formulations of lattice fermions is its exact chiral symmetry, which strongly constrains patterns in the spectrum – zero modes are chiral, nonzero eigenvalue modes are not. This spares a lot of argument about how lattice artifacts affect results. (For example, is a small eigenvalue eigenmode an approximation to a true zero mode, or not?) An issue with the program is that in the epsilon regime, finite size corrections are power law in  $1/L$ , rather than exponential ( $\exp(-m_\pi L)$ ) as they are for conventional measurements. In the end, large volumes were needed to overcome these large corrections.

Studies of hadronic observables in the “p-regime” ( $m_\pi L \gg 1$ ) are done basically identically to the ones using nonchiral actions. Many auxiliary calculations which one would do with a nonchiral fermion (clover or Wilson), such as the determination of an additive shift in the fermion mass or separate evaluations of  $Z$ -factors of quantities related by chiral rotations, become unnecessary (except as checks that things have been coded correctly).

The awkward struggles between flavor and taste so typical of staggered fermion calculations are simply absent, too. I found that this simplified my analysis of data in the projects I did.

Of course, the Dirac propagator is the work horse of nearly all QCD calculations. A flowchart of the construction of  $\hat{D}(m)^{-1}\chi$  goes as follows: Temporarily label  $C = 1 - m^2/(4r_0/a)^2$ ,  $S = m^2/C$ . Then

1. Solve for  $\psi = (H^2 + S)^{-1}\chi$  using your favorite sparse matrix inversion routine.
2. Before subtraction, compute

$$D^{-1}\chi = D(m)^\dagger[H(m)]^{-2}\chi = \frac{1}{C}[(1 - \frac{m}{2r_0/a})H\gamma_5 + m]\psi. \quad (4.13)$$

3. Then the subtracted inverse Dirac operator (Eq. 2.16) is

$$\hat{D}^{-1}\chi = \frac{1}{1 - \frac{m}{2r_0/a}}[D^{-1}\chi - \frac{1}{2r_0/a}\chi]. \quad (4.14)$$

It is useful to precondition the inversion using eigenmodes of  $H$ , if they are available.

Now for a few words about simulations with dynamical overlap fermions. All the projects I know of used hybrid Monte Carlo (HMC) with the  $\Phi$  hybrid molecular dynamics (MD) algorithm. The  $\Phi$  algorithm obtains the force on the gauge field from the derivative of the pseudofermion effective potential  $S_f = \Phi^*[M(U)^\dagger M(U)]^{-1}\Phi$  with respect to the vector potential  $A$  or  $U$ . Because the fermion matrix depends on the gauge field, the pseudofermion term contributes the “fermion force”,

$$iF_{F,\mu\nu} = X^* \frac{\partial}{i\partial A_{\mu\nu}} [M(U)^\dagger M(U)] X. \quad (4.15)$$

As long as  $M(U)$  changes smoothly with  $U$  there is no problem evaluating this expression and one proceeds as one does in simulations with some conventional fermion discretization. As we move along the molecular dynamics trajectory, however, one of the eigenvalues of the kernel operator might change sign, signaling the appearance or disappearance of a zero mode. The topology of the underlying gauge configuration (as seen by the fermions) is trying to change. When that occurs, the spectrum of the overlap operator  $M(U)$  changes discontinuously. This discontinuity generates an infinite fermion force. Conventional MD stepping algorithms, such as the leapfrog, fail, and special treatment is called for. In particular we need a reversible MD treatment to carry us past the step.

A reversible molecular dynamics treatment of a discontinuous effective potential was proposed by [26]. It is based on the analogy with classical particle motion in the presence of a step barrier. Imagine a unit-mass particle moving in two spatial dimensions  $(x, y)$ , and approaching a potential step, with  $V(x, y) = 0$ , say, for  $x < 0$  and  $V(x, y) = V_0$  for  $x > 0$ . The component of momentum in the  $y$  direction is unchanged when the particle strikes the barrier, but there is an impulse in the  $x$  direction, which causes a discontinuous change in  $p_x$ . If the barrier is too high, the particle “reflects,”  $p_x \rightarrow -p_x$ , but if the barrier is low enough, the particle crosses the barrier (“refracts”) while  $p_x$  changes. The change is given by energy conservation,  $\frac{1}{2}p_x^2 = \frac{1}{2}(p'_x)^2 + V_0$ .

In the QCD simulation, we need to identify the Molecular Dynamics time at which one of the eigenmodes of the kernel operator has a zero eigenvalue. We move along the

trajectory monitoring the eigenvalues of  $h$  until we arrive at that “crossing” time. (This is not an extra expense, if eigenmodes of  $h$  are being used to precondition the evaluation of  $\epsilon(h)$ .) If we step “across the boundary,” so the minimum  $\lambda$  changes sign, we have to go back and adjust the integration step size until we land precisely on  $\lambda = 0$ . Then we change the gauge field momentum  $P$  discontinuously, reflecting or refracting according to the size of the step in the potential  $\Delta S_f$ . After reflecting or refracting, we return to our usual leapfrog integration until the end of the trajectory (or until we reach the next topological boundary).

Recall that the analog of the energy was  $\frac{1}{2}P^2 + S$ . In terms of the unit normal vector to the surface of discontinuity  $N$ , there are two possibilities for changes in the gauge momenta, depending on the size of the momentum component along the normal.

In compact notation we denote the inner product of two vector fields in the Lie algebra of  $SU(N)$  by

$$N^*P = \sum_{n\mu} \text{Tr}(N_{n\mu}^\dagger P_{n\mu}) . \quad (4.16)$$

Then, if  $(N^*P)^2 > 2\Delta S_f$ , we have refraction:

$$\Delta P = -N (N^*P) + N \text{sign}(N^*P) \sqrt{(N^*P)^2 - 2\Delta S_f}. \quad (4.17)$$

Alternatively, if  $(N^*P)^2 \leq 2\Delta S_f$ , we have reflection:

$$\Delta P = -2N(N^*P). \quad (4.18)$$

Here  $\Delta S_f$  is the height of the discontinuity, which only arises from the fermionic part of the action. It happens because one eigenvalue of the kernel action  $h$  changes sign. (Recall Eq. (4.5).) Calling this eigenvector  $\chi$ , the (unnormalized) normal vector  $N$  is the matrix element of the derivative of the kernel action with respect to  $A$ , computed in this special crossing state

$$N(x, \mu) = \chi^* \frac{\partial h}{\partial A(x, \mu)} \chi. \quad (4.19)$$

In practice, the exact step function of the overlap operator is replaced by some approximation, such as a rational functional approximation. To obtain an accurate approximation to the step function, it continues to be necessary to project out low modes of the kernel operator, as in Eq. (4.5). This introduces another complication for HMC: we have to be able to differentiate the projector. Evaluating the derivative requires determining the change in the projector under small perturbations in  $h$ . Labeling the projector on an eigenmode of  $h(-r0)$  with eigenvalue  $\lambda$  as  $P_\lambda = |\lambda\rangle\langle\lambda|$ , first order perturbation theory gives [27]

$$\delta P_\lambda = \frac{1}{\lambda - h} (1 - P_\lambda) \delta h P_\lambda + P_\lambda \delta h \frac{1}{\lambda - h} (1 - P_\lambda). \quad (4.20)$$

In the force, this term is combined with an analytic differentiation of the rational functional approximation, using sources from which the low modes have been projected out, basically a mix of Eqs. (4.15) and (4.5).

All this business with reflection and refraction is morally equivalent to the problem of changing topology as seen in simulations with actions which treat topology only approximately (meaning, everything else but overlap fermions). What is different is that here, the barrier between topology changes is sharp and easy to understand. As with other actions,

simulations with overlap fermions have a hard time changing topology and the problem gets worse as the lattice spacing decreases. It is very easy, though, to perform simulations in sectors of fixed topology, simply by always reflecting from topological boundaries. These data sets can be used in the epsilon regime studies described above, to check predictions for the properties of eigenvalues in sectors of fixed winding number.

The magical properties of overlap fermions allow simulations of an odd number of flavors without rooting. For details, see Ref. [28].

Finally, let me make a few remarks about my own experiences with the overlap as a computational problem. (This is described in more detail in Ref. [29].) I was never able to get anything useful out of an overlap operator whose kernel  $d$  or  $h$  was a usual Wilson fermion with thin links. It was too expensive to evaluate;  $\epsilon_N$  needed very large  $N$  and very small  $c_{2l-1}$ 's. The issue, I always thought, was that while the spectrum of the overlap  $D$  was a circle, that was not the case for the kernel Wilson action. (An example was shown in Fig. 1.) I always felt that it was asking a lot of the computer to map the crosses in Fig. 1 onto the Ginsparg-Wilson circle. Actions with nearest neighbor and diagonal ( $\pm\hat{i}\pm\hat{j}$ ) couplings produced approximately circular spectra to start with, and it was easier for the overlap operator to circularize them. Smearing gauge connections plus a clover term further smoothed the action and allowed me to use an  $\epsilon_N$  with small  $N$  and a more well-behaved range of eigenvalues of  $h$ . I used eigenmodes of  $h$  to precondition the calculation of  $H$  and eigenmodes of  $H$  to precondition the calculation of  $\hat{D}^{-1}$ .

Looking back, I am not sure that I found the most efficient algorithm. Every paper in the literature using overlap fermions in a QCD context has its own long set of tricks to tame the overlap and make it manageable. Nothing ever produced an action which was less than about 50 times as expensive (in terms of the cost to calculate  $\psi = D\chi$ ) as the equivalent cost for a nonchiral action.

## V. FINAL THOUGHTS

At the end of this note I feel like I have mostly been writing about a fascinating theoretical development which was a computational dead end.

A crude way to do history is to look up an article on the Inspire (<https://inspirehep.net>) data base. The articles posted there come with a histogram showing the number of citations per year. One can mark the “end of a subject” by the time when the mean number of citations per year falls below one, and the histogram breaks up into separate blocks. For most of the overlap literature, that date is before 2015.

As far as I can tell from a literature search, only one lattice group doing large scale simulations used overlap fermions (though there were several groups doing small scale simulations). That was JLQCD, who started carrying out  $N_f = 2$  flavor simulations around 2006, with a  $16^3 \times 32$  volume and quark masses down to a nominal 20 MeV or  $m_q = m_{strange}/6$  – see Ref. [30]. A year later they were doing  $N_f = 2 + 1$  flavor simulations. Their overlap program continued until about 2014, at which point they converted to simulating Moebius domain wall fermions [31]. These fermions do not have exact chiral symmetry, but the additive mass renormalization they observed was about 1/2 MeV, which they argued was more than adequate for their needs.

Advances in techniques also rendered many of the theoretical advantages of exact chiral symmetry less important. For example, these days the topological susceptibility can be measured using gradient flow [32] from simulations with nonchiral fermion actions, rather

than by counting zero modes. The condensate can be measured from the integrated spectral density of eigenvalues of a (nonchiral) Dirac operator [33]. And of course, most of the “classic problems” from the time of the development of the overlap have been solved: measurements of the condensate or the pseudoscalar decay constant are not so newsworthy any more. Groups have moved on to more complicated observables, where many things have to be balanced against each other – small lattice spacing, large volume, large statistics, multiparticle correlation functions, good chiral symmetry properties, and more.

I think that the organizers of this collection of articles wanted a small section about the overlap because it represents an aspirational ideal: it is possible to encode a version of chiral symmetry in a lattice fermion formulation which is exact even at nonzero lattice spacing.

And as we leave this review we can also leave QCD for a bigger question: is it possible to construct a lattice-regulated chiral gauge theory and thereby have a nonperturbative formulation of the Standard Model? This has been an open problem for most of the lifetime of lattice QCD. Much of the literature in this field starts with modifications to domain wall or overlap fermions. Perhaps the overlap story is not over quite just yet.

## ACKNOWLEDGMENTS

Most of what I learned about Ginsparg-Wilson fermions came via my collaborations with Anna Hasenfratz, Peter Hasenfratz, Ferenc Niedermayer, and Stefan Schaefer. I particularly want to say how much I learned from Peter Hasenfratz; I remember how hard I worked to keep up with him. He was a great physicist and a good person.

- 
- [1] H. B. Nielsen and M. Ninomiya, Absence of Neutrinos on a Lattice. 1. Proof by Homotopy Theory, Nucl. Phys. B **185**, 20 (1981), [Erratum: Nucl.Phys.B 195, 541 (1982)].
  - [2] H. B. Nielsen and M. Ninomiya, Absence of Neutrinos on a Lattice. 2. Intuitive Topological Proof, Nucl. Phys. B **193**, 173 (1981).
  - [3] L. H. Karsten and J. Smit, Lattice Fermions: Species Doubling, Chiral Invariance, and the Triangle Anomaly, Nucl. Phys. B **183**, 103 (1981).
  - [4] P. H. Ginsparg and K. G. Wilson, A Remnant of Chiral Symmetry on the Lattice, Phys. Rev. D **25**, 2649 (1982).
  - [5] M. Luscher, Exact chiral symmetry on the lattice and the Ginsparg-Wilson relation, Phys. Lett. B **428**, 342 (1998), arXiv:hep-lat/9802011.
  - [6] M. E. Peskin and D. V. Schroeder, *An Introduction to quantum field theory* (Addison-Wesley, Reading, USA, 1995).
  - [7] P. Di Vecchia and G. Veneziano, Chiral Dynamics in the Large n Limit, Nucl. Phys. B **171**, 253 (1980).
  - [8] H. Leutwyler and A. V. Smilga, Spectrum of Dirac operator and role of winding number in QCD, Phys. Rev. D **46**, 5607 (1992).
  - [9] R. J. Crewther, Chirality Selection Rules and the U(1) Problem, Phys. Lett. B **70**, 349 (1977).
  - [10] F. Niedermayer, Exact chiral symmetry, topological charge and related topics, Nucl. Phys. B Proc. Suppl. **73**, 105 (1999), arXiv:hep-lat/9810026.
  - [11] H. Neuberger, Exactly massless quarks on the lattice, Phys. Lett. B **417**, 141 (1998), arXiv:hep-lat/9707022.

- [12] H. Neuberger, A Practical implementation of the overlap Dirac operator, *Phys. Rev. Lett.* **81**, 4060 (1998), arXiv:hep-lat/9806025.
- [13] P. Hernandez, K. Jansen, and M. Luscher, Locality properties of Neuberger's lattice Dirac operator, *Nucl. Phys. B* **552**, 363 (1999), arXiv:hep-lat/9808010.
- [14] M. Luscher, Chiral gauge theories revisited, *Subnucl. Ser.* **38**, 41 (2002), arXiv:hep-th/0102028.
- [15] N. I. Akhiezer, *Theory of approximation* (Dover Publications, New York, USA, 2003).
- [16] N. I. Akhiezer, *Elements of the theory of elliptic functions* (American Mathematical Society, New York, USA, 1990).
- [17] W. H. Press, S. A. Teukolsky, W. T. Vetterling, and B. P. Flannery, *Numerical Recipes in C: The Art of Scientific Computing* (Cambridge University Press, New York, USA, 1988).
- [18] T. Kalkreuter and H. Simma, An Accelerated conjugate gradient algorithm to compute low lying eigenvalues: A Study for the Dirac operator in SU(2) lattice QCD, *Comput. Phys. Commun.* **93**, 33 (1996), arXiv:hep-lat/9507023.
- [19] A. Stathopoulos, Nearly optimal preconditioned methods for hermitian eigenproblems under limited memory. part i: Seeking one eigenvalue, *SIAM Journal on Scientific Computing* **29**, 481 (2007), <https://doi.org/10.1137/050631574>.
- [20] A. Stathopoulos and J. R. McCombs, Nearly optimal preconditioned methods for hermitian eigenproblems under limited memory. part ii: Seeking many eigenvalues, *SIAM Journal on Scientific Computing* **29**, 2162 (2007), <https://doi.org/10.1137/060661910>.
- [21] J. Gasser and H. Leutwyler, Light Quarks at Low Temperatures, *Phys. Lett. B* **184**, 83 (1987).
- [22] J. Gasser and H. Leutwyler, Thermodynamics of Chiral Symmetry, *Phys. Lett. B* **188**, 477 (1987).
- [23] E. V. Shuryak and J. J. M. Verbaarschot, Random matrix theory and spectral sum rules for the Dirac operator in QCD, *Nucl. Phys. A* **560**, 306 (1993), arXiv:hep-th/9212088.
- [24] P. H. Damgaard, The Microscopic Dirac operator spectrum, *Nucl. Phys. B Proc. Suppl.* **106**, 29 (2002), arXiv:hep-lat/0110192.
- [25] S. Aoki *et al.* (Flavour Lattice Averaging Group), FLAG Review 2019: Flavour Lattice Averaging Group (FLAG), *Eur. Phys. J. C* **80**, 113 (2020), arXiv:1902.08191 [hep-lat].
- [26] Z. Fodor, S. D. Katz, and K. K. Szabo, Dynamical overlap fermions, results with hybrid Monte Carlo algorithm, *JHEP* **08**, 003, arXiv:hep-lat/0311010.
- [27] R. Narayanan and H. Neuberger, An Alternative to domain wall fermions, *Phys. Rev. D* **62**, 074504 (2000), arXiv:hep-lat/0005004.
- [28] T. DeGrand and S. Schaefer, Simulating an arbitrary number of flavors of dynamical overlap fermions, *JHEP* **07**, 020, arXiv:hep-lat/0604015.
- [29] T. A. DeGrand (MILC), A Variant approach to the overlap action, *Phys. Rev. D* **63**, 034503 (2000), arXiv:hep-lat/0007046.
- [30] T. Kaneko *et al.* (JLQCD), JLQCD's dynamical overlap project, *PoS LAT2006*, 054 (2006), arXiv:hep-lat/0610036.
- [31] J. Noaki, S. Aoki, G. Cossu, H. Fukaya, S. Hashimoto, and T. Kaneko (JLQCD), Fine lattice simulations with the Ginsparg-Wilson fermions, *PoS LATTICE2014*, 069 (2014).
- [32] M. Lüscher, Properties and uses of the Wilson flow in lattice QCD, *JHEP* **08**, 071, [Erratum: *JHEP* **03**, 092 (2014)], arXiv:1006.4518 [hep-lat].
- [33] L. Giusti and M. Luscher, Chiral symmetry breaking and the Banks-Casher relation in lattice QCD with Wilson quarks, *JHEP* **03**, 013, arXiv:0812.3638 [hep-lat].